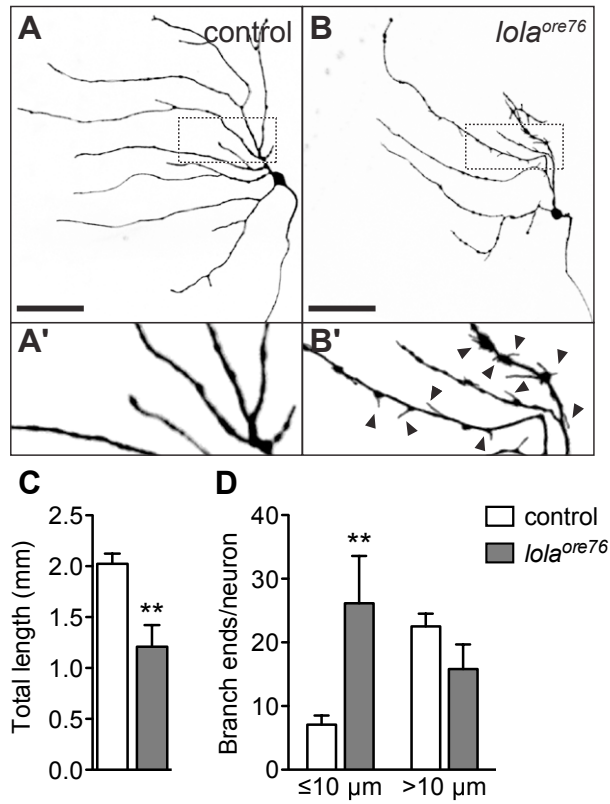
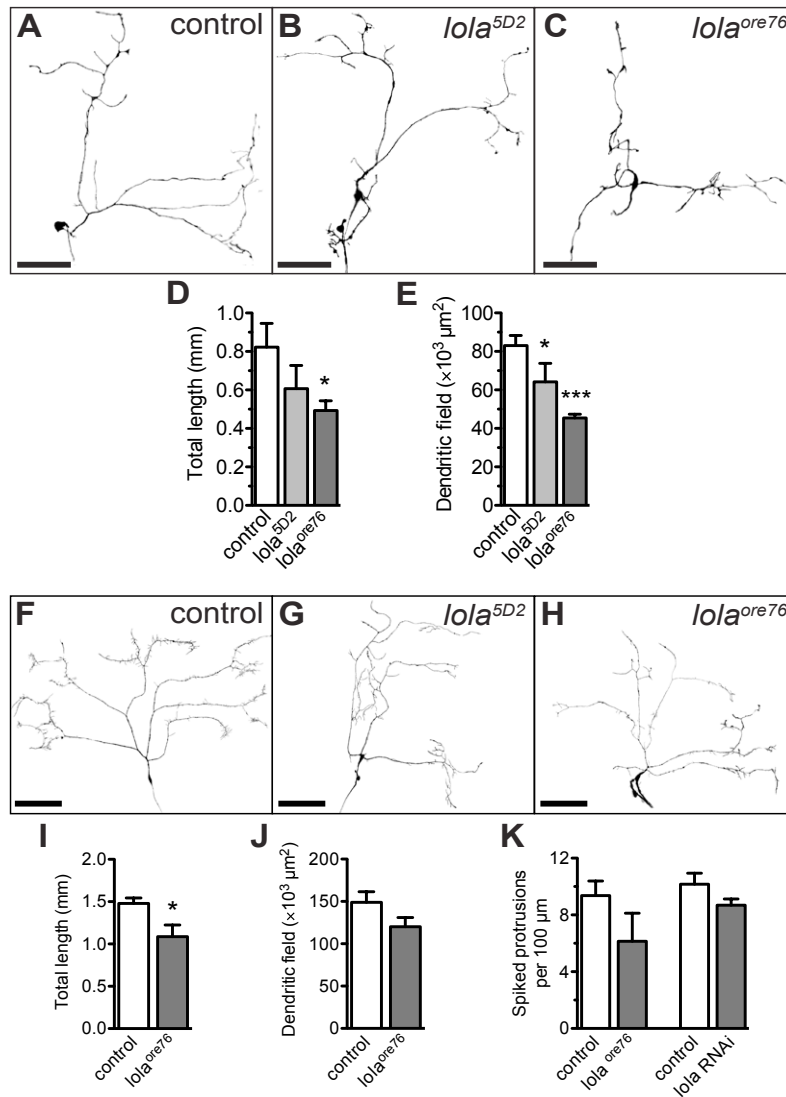


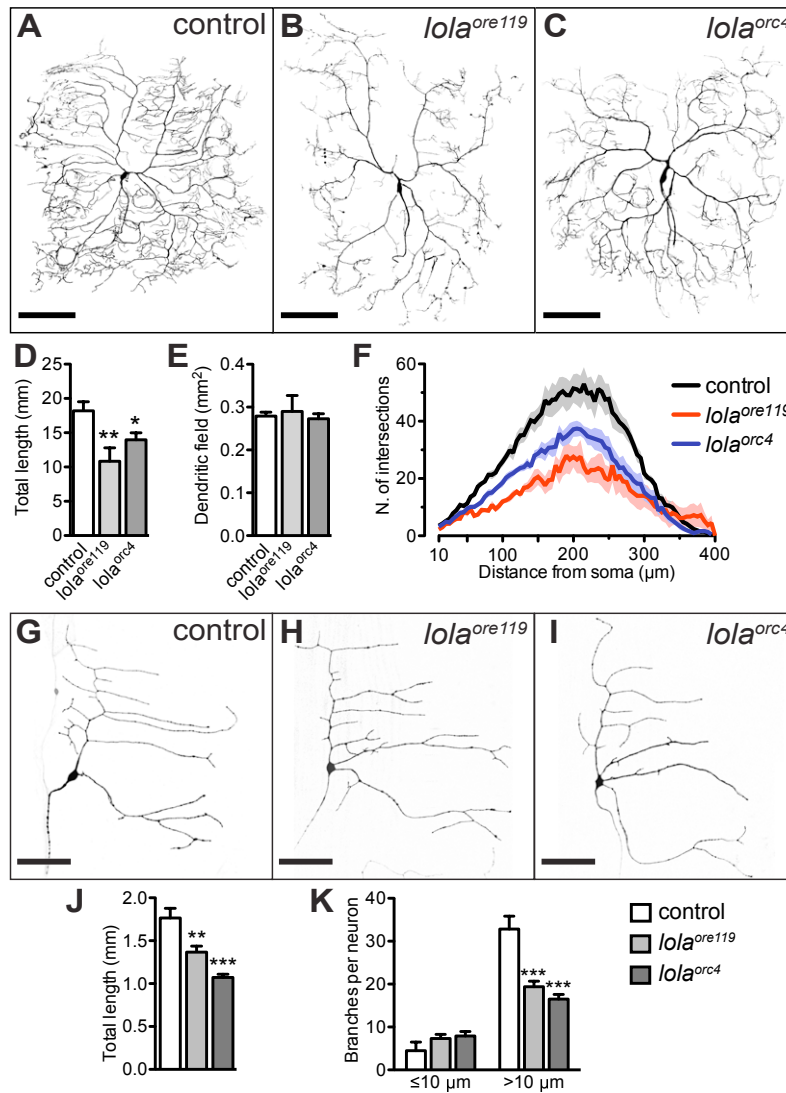
**Figure S1. Axon terminals of class IV da neurons appear unaffected by *lola* RNAi in third instar larvae.** To label axon terminals of class IV da neurons using *ppk1.9-GAL4*, we used the membrane reporter CD4::tdTomato (tdTom, magenta) or one of two reporters for presynaptic proteins: neuronal synaptotagmin (UAS-syt.eGFP, A',B'), or synaptobrevin (UAS-n-syb.eGFP, C',D'). These markers revealed no overt defects in *lola* RNAi animals. Scale bars: 25 $\mu$ m.



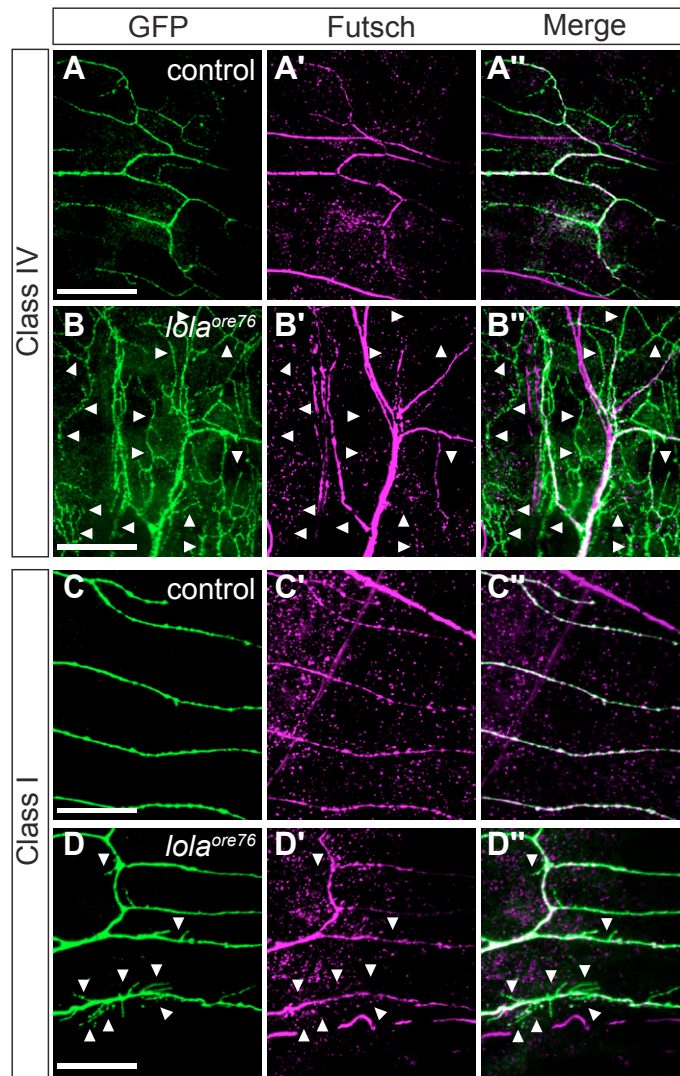
**Figure S2. Lola cell autonomously regulates dendrite growth and branching in class I ddaD neurons.** (A,B) MARCM clones of Class I ddaD neurons in controls (A) and *lola<sup>ore76</sup>* (B). Dashed boxes are enlarged in corresponding panels (A',B') to depict the numerous short branches in *lola* mutants (arrowheads). (C,D) Quantifications comparing control (N=10) and *lola<sup>ore76</sup>* (N=6) clones. (C) Total arbor length (t-test, P=0.0015). (D) Branch number per neuron below (t-test, P=0.0060) or above (t-test, P= 0.1120) a 10μm threshold. Scale bars: 50μm.



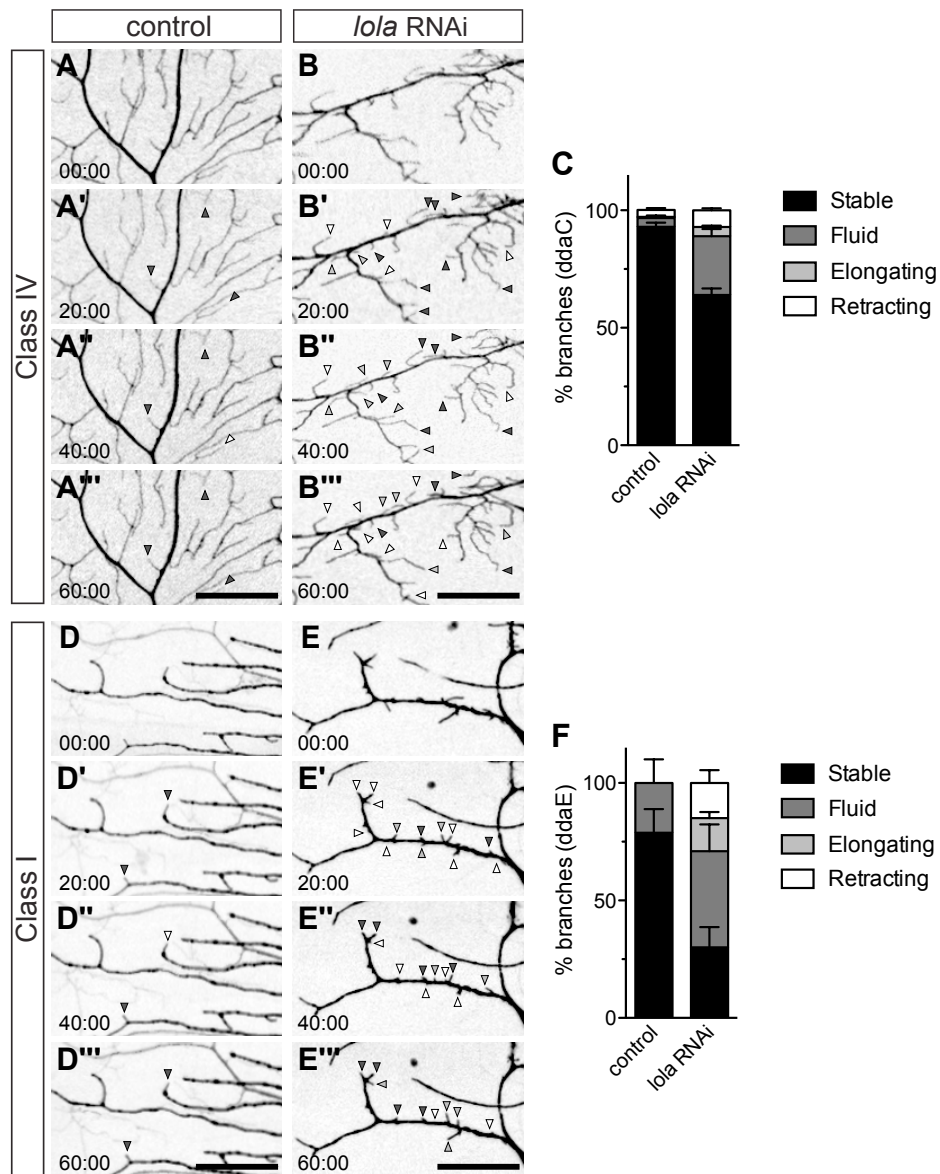
**Figure S3. Lola is required for dendrite growth in class II and III da neurons.** (A-C) MARCM clones of class II ddaB neurons. (A) Control, (B) *lola<sup>SD2</sup>* and (C) *lola<sup>ore76</sup>* ddaB clones showing reduced lengths of major branches. (D,E) Quantifications comparing ddaB controls (N= 7), *lola<sup>SD2</sup>* clones (N= 3), and *lola<sup>ore76</sup>* clones (N= 9). (D) Total arbor length (ANOVA,  $F_{2,16} = 3.745$ ,  $P = 0.0463$ ). (E) Dendritic field (ANOVA,  $F_{2,16} = 22.48$ ,  $P < 0.0001$ ). (F-K) MARCM clones of class III ddaF neurons. (F) Control, (G) *lola<sup>SD2</sup>* and (H) *lola<sup>ore76</sup>* ddaF clones showing decreased arbor length. (I-K) Quantifications comparing ddaF controls (N= 10) and *lola<sup>ore76</sup>* MARCM clones (N= 4). (I) Total arbor length (t-test,  $P = 0.0419$ ). (J) Dendritic field (t-test,  $P = 0.1307$ ). (K) In class III neurons, the density of the spiked protrusions that characterize these arbors was not significantly affected in ddaF MARCM clones (t-test,  $P = 0.136$ ), nor in ddaA knockdown cells (UAS-*lola*RNAi driven by *tut1<sup>GAL4</sup>*, a class III specific driver; controls: N= 15, *lola* RNAi: N= 15; t test,  $P = 0.1056$ ). Scale bars: 100  $\mu\text{m}$ .



**Figure S4. Specific mutations of Lola isoforms L or K reduce dendritic arbors of class IV and class I neurons.** (A-F) MARCM clones of the class IV neuron ddaC. (A) Control, (B) *lola<sup>ore119</sup>* (a mutation in isoform L) and (C) *lola<sup>orc4</sup>* (a mutation in isoform K) clones. (D-F) Quantifications comparing ddaC controls (N= 12), *lola<sup>ore119</sup>* clones (N= 5), and *lola<sup>orc4</sup>* clones (N= 9). (D) Total arbor length (ANOVA,  $F_{2,23} = 9.032$ ,  $P = 0.0013$ ). (E) Dendritic field (ANOVA,  $F_{2,23} = 0.2666$ ,  $P = 0.7683$ ). (F) Sholl profiles. (G-I) MARCM clones of the class I neuron ddaE. (J,K) Quantifications comparing ddaE controls (N= 8), *lola<sup>ore119</sup>* clones (N= 13), and *lola<sup>orc4</sup>* clones (N= 10). (J) Total arbor length (ANOVA,  $F_{2,28} = 22.18$ ,  $P < 0.0001$ ). (K) Branch number per neuron below (ANOVA,  $F_{2,28} = 1.365$ ,  $P = 0.276$ ) or above ( $F_{2,28} = 23.04$ ,  $P < 0.0001$ ) a 10μm threshold. Scale bars: A-C: 100μm; G-I: 50μm.



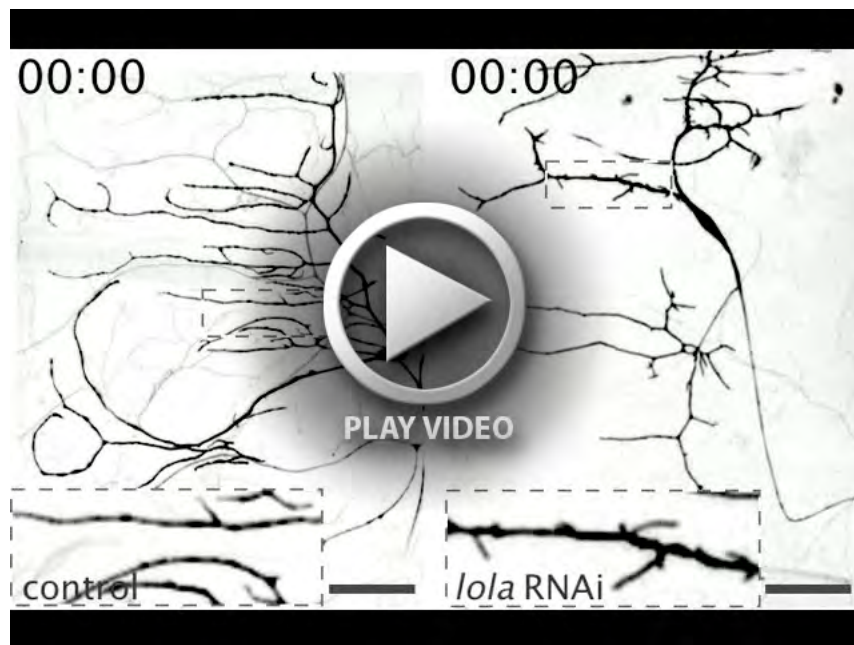
**Figure S5. Stable microtubules were virtually absent in ectopic branches of *lola* mutant neurons.** (A,B) MARCM clones of class IV ddaC neuron showing distal branches of a control neuron (A) and the proximal bushy arbor of a *lola<sup>ore76</sup>* clone (B). (A',B') Futsch immunoreactivity was detected in the distal branches of control neuron (A') as well as the proximal thicker arbors of *lola<sup>ore76</sup>* clone (B'), but was absent from the numerous thinner branches in *lola<sup>ore76</sup>* (B', arrowheads). (A'',B'') Overlay of GFP and Futsch channels. (C,D) MARCM clones of class I ddaE neuron showing details of the dendritic branches. (C',D') Futsch immunoreactivity was detected in the main branches of both control (C') and *lola<sup>ore76</sup>* (D') ddaE neuron, but was undetectable in the short branches of *lola<sup>ore76</sup>* neuron (D', arrowheads). (C'', D'') Overlay of GFP (green) and Futsch (magenta) channels. Scale bars: 25 $\mu$ m.



**Figure S6. Lola suppresses branch stabilization in late third instar larvae.** Branching dynamics revealed by time-lapse confocal images of proximal arbors of late third-instar larvae at 5 min intervals (for simplicity, only every 4<sup>th</sup> frame is shown). (A-C) Class IV ddaC neurons. (A-A''') The majority of branch ends in the proximal region of control larva (*UAS-Dcr2;ppk1.9-GAL4,ppk-CD4::tdTomato*) are stable over the period of one hour. (B-B''') In contrast, dendrites in *lola* RNAi larvae (*UAS-Dcr2;UAS-RNAi;ppk1.9-GAL4,ppk-CD4::tdTomato*) exhibit multiple dynamic branching events, including retractions (white arrowheads), extensions (light gray arrowheads), and fluid branches that both extend and retract (dark gray arrowheads). (C) Relative percentages of stable and dynamic branching events, with nearly 1.5 fold reduction in the frequency of stable branches in *lola* RNAi ( $63.92 \pm 3.95$ ) when compared to controls  $90.55 \pm 2.37$ ). (D-F) Class I ddaE neurons. The numerous short branches in *lola* RNAi are highly dynamic, with nearly threefold reduction in the frequency of stable branches ( $30.03 \pm 12.17$ ) when compared to controls ( $78.78 \pm 14.30$ ). N=2 larvae for each genotype. Scale bars: 25 $\mu$ m. The depicted time-lapses are available as supplemental movies 1 and 2.



**Movie 1. Time-lapse movie of proximal branch dynamics of ddaC class IV neurons at the third instar larval stage.** While proximal branches of a representative control larva (left panel, *UAS-Dcr2;;ppk1.9-GAL4,ppk-CD4::tdTomato*) remain stable over the imaging period, *lola* RNAi larva (right panel, *UAS-Dcr2;UAS-RNAi;ppk1.9-GAL4,ppk-CD4::tdTomato*) exhibit multiple dynamic events. The second part of the video repeats the time series while annotating the video-tracked branch ends in the image field. Stacks were acquired every 5 minutes and a maximal projection at each time point used to generate the sequence. Time-stamps are indicated on the upper-left of each panel. While the time series lasts more than one hour, quantifications were restricted to the first hour. Scale bars: 25 $\mu$ m.



**Movie 2. Time-lapse movie of proximal branch dynamics of class I neurons at the third instar larval stage.** Most branch ends remain stable in controls (left panel, *UAS-Dcr2;;GAL4<sup>221</sup>,UAS-mCD8::GFP*), but highly dynamic in *lola* RNAi (right panel, *UAS-Dcr2;UAS-RNAi;GAL4<sup>221</sup>,UAS-mCD8::GFP*) animals. Stacks were acquired every 5 minutes and a maximal projection at each time point used to generate the sequence. Time-stamps are indicated on the upper-left of each panel. Dashed boxes are enlarged in corresponding insets. While the time series lasts more than one hour, quantifications were restricted to the first hour. Scale bars: 25 $\mu$ m.